View Article Online / Journal Homepage / Table of Contents for this issue
Dynamic Article Links

Analyst

Cite this: *Analyst*, 2012, **137**, 5071

www.rsc.org/analyst

PAPER

Published on 28 August 2012. Downloaded by The University of Melbourne Libraries on 10/09/2013 11:31:13.

A simple and label-free electrochemical biosensor for DNA detection based on the super-sandwich assay†

Long Yin Zhou, Xi Yuan Zhang, Gang Lin Wang, Xiao Xia Jiao, Hong Qun Luo* and Nian Bing Li*

Received 4th July 2012, Accepted 27th August 2012
DOI: 10.1039/c2an35905g

The focus of this work was on designing a label-free DNA biosensor based on a super-sandwich assay using the electrochemical impedance spectroscopy technique. For this purpose, we designed a signal-up configuration whose linker probes could hybridize with two regions of the target DNA. In this configuration, the presented target DNA would effectively decrease the electron transfer, which would improve the sensitivity of the sensor. Ultimately, we employed gel electrophoresis to further confirm the formation of the proposed super-sandwich structure.

Introduction

The sandwich assay has become a mainstay for the detection of oligonucleotides, proteins, and small molecules.[1–11] The utility of this assay has two aspects. On the one hand, it does not require the target oligonucleotide to be fluorescent, enzymatic, or otherwise labeled.[2] On the other hand, the capture and signal probes do not come into proximity in the absence of target, which reduces the background signals, magnifies the signal change produced by target binding, and leads to often impressive detection limits. But for normal sandwich assay, each capture probe can only capture a single target molecule and signal probe, thus limiting signal intensity and sensitivity. Most recently, the 'super-sandwich' assay has been designed by Xia and co-workers.[12] Yuan and co-workers detected Pb^{2+} by a label-free super-sandwich electrochemiluminescence sensor.[13] Chen and co-workers designed a simple, ultrasensitive, and selective electrochemical DNA biosensor based on DNA concatemers, whose detection limit for target DNA can be as low as 100 aM even in complex samples.[14]

Herein we report on a new, label-free DNA biosensor for the detection of oligonucleotides based on a super-sandwich assay by the electrochemical impedance spectroscopy (EIS) technique. We designed a signal-up configuration assay. In this configuration, linker probes hybridize with two regions of the target DNA, thus creating long concatemers containing multiple target molecules and linker probes and leading to improved signal and detection limit (Fig. 1). To further confirm this phenomenon, we adopted gel electrophoresis to investigate this super-sandwich assay and the results were in good agreement with our speculation. Resulting from the advantage of the resistance change rate ΔR_{ct}, $\Delta R_{ct} = (R_{ctT} - R_{ctM})/R_{ctM}$ (R_{ctT}, resistance of added target; R_{ctM}, resistance of the modified electrode without target), the detected concentration of target can be as low as 1.7 nM. EIS is a highly sensitive technique attracting more and more attention from biologists as it has a less destructive effect on the measurement of biological interactions, owing to its very narrow range of small operation potentials. EIS measurements of the super-sandwich exploiting an external redox probe, such as $[Fe(CN)_6]^{3-/4-}$, have grown in importance.[15–17] The oligonucleotide with negative charge was self-assembled on the gold electrode, which would block the electron transfer. The more the oligonucleotide sequences were self-assembled on the gold electrode, the more difficult it would be for the electrons to approach the electrode surface. So, we can conclude that the 'super-sandwich' structure could be more effective to block the electron transfer than the traditional-sandwich structure. Consequently, a substantial

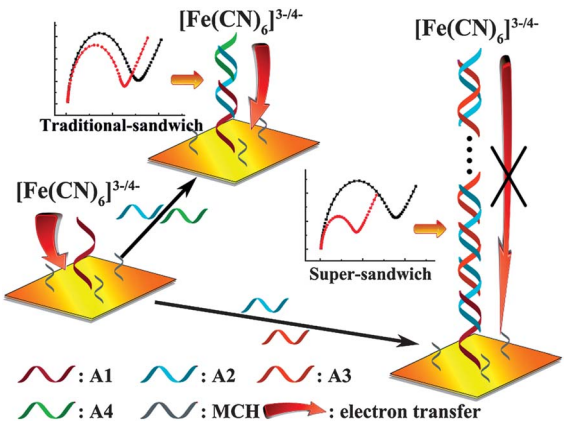

Fig. 1 A schematic illustration of the traditional-sandwich assay (top) and super-sandwich assay (right). A1 is the capture probe; A2 is the target; A3 is the linker probe of the super-sandwich; A4 is the signal probe of the traditional-sandwich.

Key Laboratory on Luminescence and Real-Time Analysis, Ministry of Education, School of Chemistry and Chemical Engineering, Southwest University, Chongqing 400715, China. E-mail: linb@swu.edu.cn; luohq@swu.edu.cn

† Electronic supplementary information (ESI) available. See DOI: 10.1039/c2an35905g

Published on 28 August 2012. Downloaded by The University of Melbourne Libraries on 10/09/2013 11:31:13.

change rate in the electron transfer resistance (ΔR_{ct}) was monitored by EIS. Based on these results, a simple and label-free electrochemical biosensor for oligonucleotide sequence was constructed. Our method is label-free and simple, which was used to detect the target without using any redox-label by the EIS technique. Compared with other redox-label electrochemical methods such as cyclic voltammetry (CV), square wave voltammetry (SWV), and differential pulse voltammetry (DPV), EIS is less destructive to the measured biological interactions because it is performed in a very narrow range of small potentials. In addition, there were no complex steps in our method, whereas in some other methods, such as employing RuHex as the signaling molecule, deoxygenation must be done *via* purging with nitrogen gas.

Experimental

Materials

All oligonucleotides used for the detection were obtained from Sangon Biotechnology Co., Ltd. (Shanghai, China) and the oligonucleotide sequences are shown as follows. Seven single strand DNA (ssDNA), which were recorded as A1 (capture probe), A2 (target), A3 (the linker probe of super-sandwich), A4 (the signal probe of traditional-sandwich), C1 (one-base mismatched target), C3 (three-base mismatched target), and C5 (five-base mismatched target), were used.

- Capture probe, A1: 5′-CCT ACC CAC ATT CTG AGA ATA CCA ACC CG–SH-3′
- Linker probe (super-sandwich), A3: 5′-CCT ACC CAC ATT CTG AGA ATA CCA ACC CG-3′
- Target, A2: 5′-AGA ATG TGG GTA GGG CGG GTT GGT ATT CT-3′
- Signal probe (traditional-sandwich), A4: 5′-GAG AAT ACC AAC CCG-3′
- 1-Mismatch target, C1: 5′-AGA ATG TGG CTA GGG CGG GTT GGT ATT CT-3′
- 3-Mismatch target, C3: 5′-AGA ATG TCC CTA GGG CGG GTT GGT ATT CT-3′
- 5-Mismatch target, C5: 5′-AGA ATC ACC CTA GGG CGG GTT GGT ATT CT-3′

Tris(2-carboxyethyl) phosphine (TCEP), NaCl, $MgCl_2 \cdot 6H_2O$, $K_3[Fe(CN)_6]$, $K_4[Fe(CN)_6] \cdot 3H_2O$, $Na_2HPO_4 \cdot 12H_2O$, $NaH_2PO_4 \cdot 2H_2O$, and 6-mercapto-1-hexanol (MCH) were purchased from Sigma (St. Louis, MO) and used as received without further purification. The solutions in the experiment were as follows: the DNA immobilization buffer containing 20 mM Tris–HCl, 100 mM NaCl, and 10 mM $MgCl_2$ (pH 7.4, 25 °C); the hybridization buffer containing 20 mM Tris–HCl, 500 mM NaCl, and 10 mM $MgCl_2$ (pH 7.4, 25 °C). The external redox probe $[Fe(CN)_6]^{3-/4-}$ solution (5 mM) was prepared with 100 mM phosphate buffer (pH 7.4, 25 °C). The solvent used for the preparation of MCH was ultrapure water. All solutions were prepared using ultrapure water (specific resistance of 18.2 MΩ cm).

Monolayer preparation

A gold electrode (2.0 mm diameter, CHI Co., Ltd., Shanghai, China) was prepared by polishing it for 3 min with a micro cloth coated with a suspension of 0.3 μm γ-alumina (Buehler) followed by polishing it for 3 min with a second micro cloth coated with a suspension of 0.05 μm γ-alumina (Buehler). The polished electrode was sonicated for 3 min in ultrapure water, ethanol, and ultrapure water to remove any remaining polishing agent. Subsequently, the gold electrode was electrochemically cleaned in 0.5 M H_2SO_4 by redox cycling and drying with nitrogen. The freshly cleaned gold electrode was incubated in 0.5 μM A1 solution (a mixture of 1 μl of 100 μM A1 with 2 μl of 10 mM TCEP in a 1.5 ml micro centrifuge tube for 60 min at room temperature (25 °C) to reduce the disulfide bond of the probe DNA) containing 20 mM Tris–HCl immobilization buffer (pH 7.4) for 16 h at room temperature. The electrode was then washed with ultrapure water for 30 s to remove any excess probe DNA physically adsorbed on the electrode surface before transferring immediately to 2 mM 6-mercaptohexanol solution for 2 h at room temperature. Prior to use, the treated electrode was rinsed with ultrapure water. For target DNA detection, the prepared electrode was immersed in 20 mM Tris–HCl hybridization buffer containing various concentrations of target DNA and the fixed concentration of linker probe for 4 h at room temperature.

Electrochemical measurements

All electrochemical experiments were performed on an elsectrochemical workstation (CHI 660D, CH Instruments, Chenhua Corp, Shanghai, China) at room temperature (25 °C) using a conventional three-electrode cell with the modified gold electrode as the working electrode, a platinum wire as the counter electrode, and an Ag/AgCl reference electrode. The reference electrode was constructed by sealing the Ag/AgCl wire into a glass tube with 3 M KCl solution that was capped with a Vycor tip. And the cell was enclosed in a grounded Faraday cage. Voltage frequencies used for EIS measurements ranged from 10 kHz to 100 mHz, and the ac voltage amplitude was 5 mV. A 10 mM $K_3[Fe(CN)_6]$–$K_4[Fe(CN)_6]$ (1 : 1) mixture in 0.1 M phosphate buffer (pH 7.4) was used as a redox probe at the formal potential of the system. All measurements were repeated for a minimum of three times with a separate electrode to obtain statistically meaningful results and a Nyquist plot (Z_{re} *vs.* Z_{im}) was drawn to analyze the impedance results.

Gel electrophoresis

Electrophoresis analysis was performed by putting the samples on a 3% gelose gel in a 1× TAE buffer (40 mM Tris acetate, 2 mM EDTA, pH 8.5) followed by electrophoresis for 40 min at 60 V. After ethidium bromide staining, the gel was imaged using a GelDoc 2000 system (BIO-RAD, USA).

Results and discussion

Difference between the super-sandwich and traditional-sandwich structures

To demonstrate that the super-sandwich sequence was more sensitive than the traditional-sandwich sequence, we measured each ΔR_{ct} of the two sequences with the same concentration of A2 (1 μM) and A3 (1 μM). As shown in Fig. 2, the ΔR_{ct} of the super-sandwich sequence was more than 3 times that of the traditional-sandwich sequence.

 This journal is © The Royal Society of Chemistry 2012

Published on 28 August 2012. Downloaded by The University of Melbourne Libraries on 10/09/2013 11:31:13.

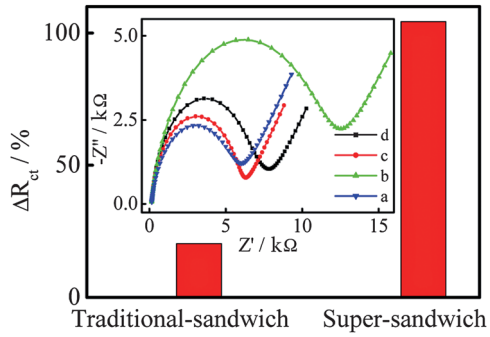

Fig. 2 Difference between the traditional-sandwich and the super-sandwich sequences. Inset: representative Nyquist plots ($-Z''$ *vs.* Z') for films of super-sandwich and traditional-sandwich. (a) Modified electrode of super-sandwich; (b) films of super-sandwich after adding target; (c) the modified electrode of traditional-sandwich; (d) films of traditional-sandwich after adding target.

Ionic strength and hybridization time

We discussed the influence of ionic strength on the hybridization of A2 (1 μM) and A3 (1 μM) on the modified gold electrode, and the results are shown in Fig. 3(A). Bar charts 1–4 represent different ionic strengths which were various concentrations of NaCl solutions (100, 300, 500, and 1000 mM) containing 20 mM Tris–HCl and 10 mM $MgCl_2$. The largest ΔR_{ct} was observed at the concentration of 500 mM NaCl. Therefore, we chose the hybridization buffer containing 20 mM Tris–HCl, 500 mM NaCl, and 10 mM $MgCl_2$ (pH 7.4, 25 °C).

Hybridization time of the target was optimized by EIS measurement at various time points (0.5, 2, 4, 6, and 16 h) during the incubation of 1 μM A2 (target) and 1 μM A3. After measurements, we calculated the relative difference in ΔR_{ct} for each target at each time point. We can observe that the ΔR_{ct} in Fig. 3(B) rapidly increased with increasing hybridization time up to 4 h and remained stable after that. Typically, we incubated the sensors for 4 h to allow the sensors to reach signal saturation.

EIS based on super-sandwich DNA-sensor

Detection of the target was verified by EIS studies on the super-sandwich system without the use of any redox marker. EIS is very sensitive to the changes in interfacial impedance of the electrodes (conductor or semiconductor) upon biorecognition events occurring at the surface–electrolyte interface.[18] EIS results were presented by the Nyquist plots, imaginary impedance $Z''(\omega)$ *vs.* real impedance $Z'(\omega)$. The impedance data were analyzed on the basis of the Vorotyntsev theoretical model of a surface-confined redox system[19] that takes into account the charge transfer process at the film–electrolyte interface as well as charge diffusion through the film.

A modified Randles equivalent circuit and the fitting of one measured spectrum to the equivalent circuit are shown in Fig. 4 (and inset). Herein, R_s denotes the ohmic resistance of the electrolyte solution; $R_{e/f}$ and R_f are the electrolyte–film interface resistance and film resistance, respectively; $Q_{e/f}$ (used as a constant phase element, CPE, to improve the fitting of the experimental data) is the electrolyte–film interface capacity; Q_f is the film capacity; and Z_w is the Warburg impedance, resulting from diffusion of the redox. In our system the charge-transfer resistance of the $[Fe(CN)_6]^{3-/4-}$ redox probe, R_{ct}, is the sum total of $R_{e/f}$ and R_f. In the Nyquist plots, the diameter of the semicircle reflects the R_{ct} of the redox conversion of the electroactive marker $[Fe(CN)_6]^{3-/4-}$ on the electrode at certain applied potential. This process is strongly dependent upon any modification to the electrode surface. When a mixed monolayer of the capture probe and MCH was self-assembled on the electrode surface, the resistance value (Fig. 4, curve c) increased significantly compared with that of the gold electrode without self-assembling anything (Fig. 4, curve a). The increase in resistance may be due to the fact that the negative charges on the phosphate backbone of the surface-immobilized probes repel $[Fe(CN)_6]^{3-/4-}$ from the electrode and backfilling of MCH for potential pinholes blocks the electron transfer. In this step, the resistance decreased (curve c) after assembly of MCH compared with curve b in Fig. 4. We may speculate that it resulted from non-specific adsorption of DNA. In the research of Schreiner and co-workers,[20] the structure and stability of single- and double-stranded DNA hybrids immobilized on gold were strongly affected by nucleotide–surface interactions. The Au–S bond is more stable than the non-specific adsorption between the DNA and gold electrode surface. After assembling the A1, some A1 molecules were non-specifically

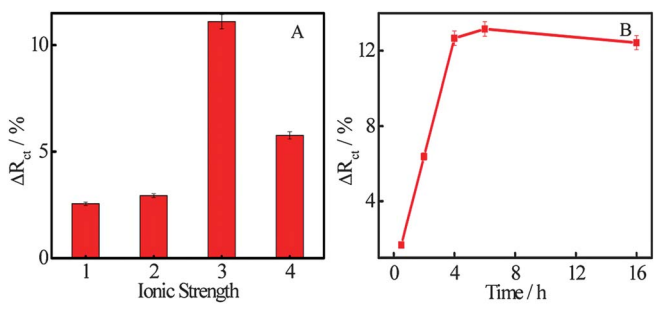

Fig. 3 (A) Relationship between EIS increase and ionic strength. Bar charts 1–4 represent various concentrations of NaCl (100, 300, 500, and 1000 mM) containing 20 mM Tris–HCl and 10 mM $MgCl_2$ (pH 7.4, 25 °C). (B) The effect of hybridization time of target on EIS increase.

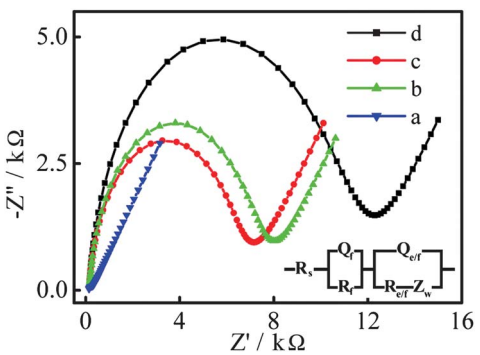

Fig. 4 Nyquist plots ($-Z''$ *vs.* Z') for super-sandwich: (a) bare gold electrode; (b) films of the capture probe A1; (c) films of assembly of A1 and MCH; (d) films of super-sandwich after adding A2 (1 μM) and A3 (1 μM). Inset: the equivalent circuit: R_s, solution resistance; $R_{e/f}$, electrolyte–film interface resistance; R_f, film resistance; $Q_{e/f}$, electrolyte–film interface capacity; Q_f, film capacity; Z_w, Warburg impedance.

Published on 28 August 2012. Downloaded by The University of Melbourne Libraries on 10/09/2013 11:31:13.

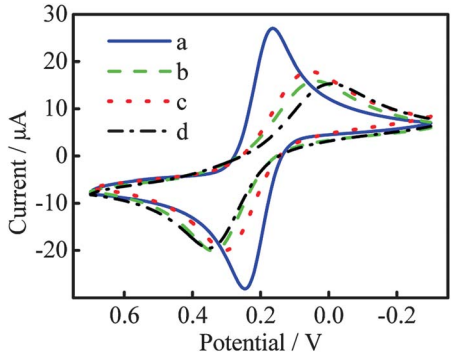

Fig. 5 CV diagrams of the biosensor at different stages: (a) bare gold electrode; (b) assembly of the capture probe A1; (c) assembly of A1 and MCH; (d) super-sandwich after adding A2 (1 μM) and A3 (1 μM).

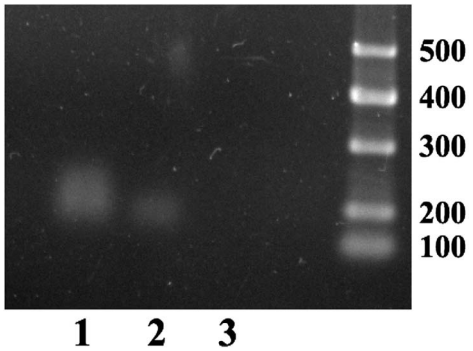

Fig. 6 The gel electrophoresis results of the super-sandwich structure. Lanes 1 and 2, which represent the super-sandwich structure with and without annealing, respectively, exhibit two ladders of super-sandwich structure, and lane 3 exhibits traditional-sandwich structure.

adsorbed on the gold electrode surface. During assembly of MCH, the A1 non-specifically adsorbed on the electrode was replaced by MCH. Because of the negatively charged phosphate backbone, the DNA molecules may be more effective than MCH to block the electron transfer. After adding A2 and A3, the resistance increased because of the super-sandwich assay (Fig. 4, curve d). The super-sandwich was repeatedly hybridized with A2 and A3. In this case, the film on the gold electrode surface increased, leading to a large increase in negative charges, which effectively blocked the electron transfer and repelled $[Fe(CN)_6]^{3-/4-}$ from the electrode surface.

Subsequently, the stepwise self-assembling procedure of the biosensor was further characterized by cyclic voltammetry, and the CV diagrams of the sensor at different stages are presented in Fig. 5, illustrating that the results were in accordance with those of the impedance test.

Demonstration of the super-sandwich assay

In the presence of the target DNA (A2), the half part of A2 can hybridize to the capture probe A1 assembled on the gold electrode. The link probe A3, which has half bases that complement the other part of A2, can hybridize to A2. The last part of A3 also can hybridize to a new target A2 just like the capture probe A1. In this structure, hybridization thus creates long concatemers containing multiple target molecules and linker probes (Fig. 1). To demonstrate the super-sandwich structure, we used gel electrophoresis analysis. We also continuously added A2 (1 μM) and A3 (1 μM) to the modified electrode every 2 h in turn, respectively, and repeated this process to observe the increase in resistance to demonstrate this structure.

The gel electrophoresis results confirmed the formation of the super-sandwich structure (Fig. 6). As we can see, two ladders of super-sandwich structure are exhibited in lanes 1 and 2 (lanes 1 and 2 represent the super-sandwich structure with and without annealing, respectively) and the maximum length is about 200–250 base pairs. Correspondingly, nothing could be observed in lane 3 exhibiting the traditional-sandwich structure. This can be attributed to the band of the traditional-sandwich with less than 50 base pairs.

To demonstrate the super-sandwich structure, we also continuously added A2 (1 μM) and A3 (1 μM) to the modified electrode to observe the change in resistance and the Nyquist plots of the results are shown in Fig. 7. The impedance of the gold electrode modified with A1 and MCH increased significantly (Fig. 7, curve b) compared with that of the bare gold electrode (Fig. 7, curve a). This is because the negative charges on the phosphate backbone of the surface immobilized probes repel $[Fe(CN)_6]^{3-/4-}$ from the electrode. After A2 and A3 with the same concentration (1 μM) were added to the modified gold electrode and hybridized for 2 h (we named this step as step 1), the resistance increased (Fig. 7, curve c), because the A1, A2, and A3 formed a double-strand DNA and more negative charges blocked the electron transfer. After step 1, we continuously added A2 and A3 to hybridize to the electrode for 2 h (we named this step as step 2). The concentrations of A2 and A3 were equal to that used in step 1. We can observe that the resistance increased again (Fig. 7, curve d), and the change of resistance is large than that in step 1. After step 2, we did step 3 which is the same as step 2. In this way, we also observed an increase in resistance, and the change of resistance in step 3 is same as that in step 2 nearly (Fig. 7, curve e). From these experimental results, we can conclude that the super-sandwich structure has been formed successfully. To demonstrate that the super-sandwich is

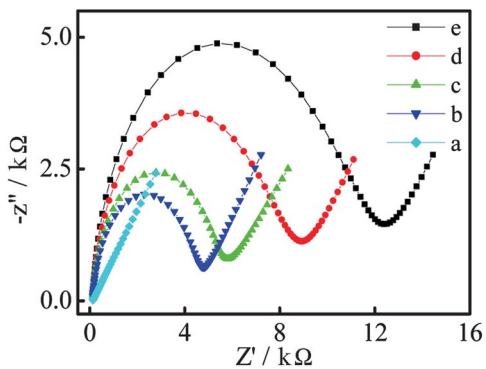

Fig. 7 Nyquist plots ($-Z''$ *vs.* Z') for demonstrating the super-sandwich structure: (a) bare gold electrode; (b) assembly of A1 and MCH; (c) step 1, the modified gold electrode after adding A2 (1 μM) and A3 (1 μM) for 2 h; (d) step 2: after step 1, A2 (1 μM) and A3 (1 μM) were added continuously for 2 h; (e) step 3: after step 2, A2 (1 μM) and A3 (1 μM) were added to the electrode for 2 h again.

This journal is © The Royal Society of Chemistry 2012

Published on 28 August 2012. Downloaded by The University of Melbourne Libraries on 10/09/2013 11:31:13.

easy to approach to the electrode, we did the experiments to prove this and the results are shown in Fig. S1 (ESI†).

Sensitivity and selectivity

The detection limit of target DNA based on this super-sandwich sequence was measured by the EIS technique. Beginning with 1 μM target DNA, ΔR_{ct} decreased with decreasing concentration of target as shown in Fig. 8. When the concentration of target gradually decreased, only a part of DNA A2 molecules could hybridize to A1 and A3 simultaneously, which led to the decrease in ΔR_{ct} until the concentration of A2 decreased to 4 nM with no change in resistance observed. Fig. 8 shows the relationship between ΔR_{ct} and the concentration of A2: ΔR_{ct} increases linearly with increasing concentration of A2 and the linear equation is $\Delta R_{ct} = 0.0920C_{A2} + 2.9027$ ($R = 0.9968$) (5 nM–1 μM). The result showed that A2 could be quantitatively measured over a large concentration range from 1 μM to 5 nM and the detection limit is 1.7 nM. In addition, we detected the target A2 by traditional-sandwich assay with EIS to obtain a linear relationship between ΔR_{ct} and the concentration of target A2 (Fig. S2, ESI†). We can observe that the super-sandwich assay is more sensitive than the traditional-sandwich assay.

The selectivity of the assay was also explored. In order to evaluate this, we challenged our assay using one-base, three-base, and five-base mismatched targets with the same concentration (400 nM) instead of the target to the sensing system as shown in Fig. 9. We found that it readily discriminates between these mismatched targets.

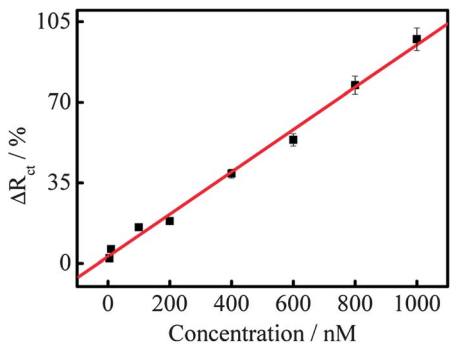

Fig. 8 Relationship between ΔR_{ct} and the concentration (5 nM–1 μM) of target DNA A2. The concentration of A3 was 1 μM; the hybridization buffer contains 20 mM Tris–HCl, 500 mM NaCl, and 10 mM $MgCl_2$ (pH 7.4, 25 °C).

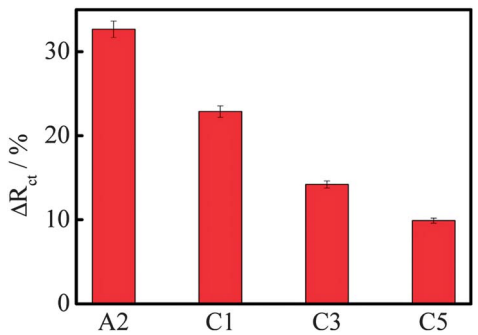

Fig. 9 Selectivity of the assay. The concentration of target A2, C1 (1-mismatch target), C3 (3-mismatch target), and C5 (5-mismatch target) was 400 nM, respectively.

Conclusion

In summary, a super-sandwich DNA conformation, induced by the oligonucleotide target, was investigated by electrochemical impedance spectroscopy, and an obvious increase in resistance was observed. The gel electrophoresis results confirmed the formation of the super-sandwich structure. Because of the advantage of resistance differences, ΔR_{ct}, the target DNA can be sensitively and selectively detected at a concentration as low as 1.7 nM. Based on these results, a simple, low-cost, and label-free electrochemical biosensor for oligonucleotide was constructed. In addition, the electrochemical approach based on the super-sandwich structure can be further extended to other DNA-based systems to detect and quantify wider ranges of analytes.

Acknowledgements

This work was supported by the National Natural Science Foundation of China (no. 20975083), and the Municipal Science Foundation of Chongqing City (no. CSTC-2008BB 4013).

References

1 Y. C. Cao, R. Jin and C. A. Mirkin, *Science*, 2002, **297**, 1536–1540.
2 T. G. Drummond, M. G. Hill and J. K. Barton, *Nat. Biotechnol.*, 2003, **21**, 1192–1199.
3 C. E. Immoos, S. J. Lee and M. W. Grinstaff, *J. Am. Chem. Soc.*, 2004, **126**, 10814–10815.
4 A. C. Syvanen and H. Soderlund, *Nat. Biotechnol.*, 2002, **20**, 349–350.
5 Y. Wan, J. Zhang, G. Liu, D. Pan, L. Wang, S. Song and C. Fan, *Biosens. Bioelectron.*, 2009, **24**, 1209–1212.
6 J. Wang, G. Liu and M. R. Jan, *J. Am. Chem. Soc.*, 2004, **126**, 3010–3011.
7 L. Wu, L. Qiu, C. Shi and J. Zhu, *Biomacromolecules*, 2007, **8**, 2795–2800.
8 J. Zhang, R. Lao, S. Song, Z. Yan and C. Fan, *Anal. Chem.*, 2008, **80**, 9029–9033.
9 J. Zhang, S. Song, L. Zhang, L. Wang, H. Wu, D. Pan and C. Fan, *J. Am. Chem. Soc.*, 2006, **128**, 8575–8580.
10 J. Y. Gerasimov and R. Y. Lai, *Chem. Commun.*, 2010, **46**, 395–397.
11 Z. Y. Lin, L. F. Chen, X. Zhu, B. Qiu and G. N. Chen, *Chem. Commun.*, 2010, **46**, 5563–5565.
12 F. Xia, R. J. White, X. L. Zuo, A. Patterson, Y. Xiao, D. Kang, X. Gong, K. W. Plaxco and A. J. Heeger, *J. Am. Chem. Soc.*, 2009, **131**, 6944–6945.
13 T. Yuan, Z. Y. Liu, L. Z. Hu, L. Zhang and G. B. Xu, *Chem. Commun.*, 2011, **47**, 11951–11953.
14 X. Chen, Y. H. Lin, J. Li, L. S. Lin, G. N. Chen and H. H. Yang, *Chem. Commun.*, 2011, **47**, 12116–12118.
15 T. H. Degefa and J. Kwak, *J. Electroanal. Chem.*, 2008, **612**, 37–41.
16 S. D. Keighley, P. Estrela, P. Li and P. Mighorato, *Biosens. Bioelectron.*, 2008, **24**, 906–911.
17 J. Y. Liu, S. J. Tian, P. E. Nielsen and W. Knoll, *Chem. Commun.*, 2005, **23**, 2969–2971.
18 E. Katz and I. Willner, *Electroanalysis*, 2003, **15**, 913–947.
19 M. A. Vorotyntsev, L. I. Daikhin and M. D. Levi, *J. Electroanal. Chem.*, 1994, **364**, 37–49.
20 S. M. Schreiner, A. L. Hatch, D. F. Shudy, D. R. Howard, C. Howell, J. L. Zhao, P. Koelsch, M. Zharnikov, D. Y. Petrovykh and A. Opdahl, *Anal. Chem.*, 2011, **83**, 4288–4295.